

# A COMPARISON OF KRIGING AND COKRIGING FOR MAPPING FOREST VOLUME IN CONNECTICUT

Susan L. King  
Operations Research Analyst  
Northeastern Research Station  
USDA Forest Service  
Newtown Square, PA 19073

Andrew J. Lister  
Forester/Geographer  
Northeastern Research Station  
USDA Forest Service  
Newtown Square, PA 19073

Michael Hoppus  
Research Forester  
Northeastern Research Station  
USDA Forest Service  
Newtown Square, PA 19073

## ABSTRACT

Ordinary kriging and cokriging are two geostatistical techniques used to create continuous maps of spatially autocorrelated attributes. Both procedures use the same primary variable, but cokriging, like multivariate statistics, incorporates additional independent variables. In this study, the primary variable is cubic foot volume and the secondary variable, mean normalized difference vegetation index, is calculated from an August 1996 Landsat Thematic Mapper satellite image. Two methods of evaluating the results include comparing the residuals and breaking both the estimated and sampled data into five volume classes and then examining the resulting confusion matrix. The comparison statistics: root mean square error, overall accuracy, and kappa statistic indicate that cokriging is superior when all of the sample data points are included. The cross-validation results show that cokriging is superior for correctly classifying the observed data by volume classes as indicated by the overall accuracy and kappa statistic. However, the cross-validation root mean square error is larger for cokriging indicating the superiority of kriging. Both procedures capture the same trends in Connecticut. Low volume areas are located around New York City and along the I-91 corridor and the high volume areas are in the NW part of the state. Kriging smoothes the map missing the fine scale heterogeneity of the landscape that cokriging detects.

## INTRODUCTION

Continuous maps of forest inventory data are in high demand because the human eye cannot always discern patterns in maps of point samples. A continuous map of cubic foot volume over a region is a desirable product as a layer in a geographical information system (GIS), a map for assisting managers interested in timber, wildlife, hydrology, and other environmental issues, and possibly as a post stratifier for statistical analysis of forest inventory data. The latter is an important issue as the USDA's Forest Inventory and Analysis units move from a periodic to an annual inventory.

The basic premise of geostatistics is that observations closer together are more similar on average than those farther apart. The most common geostatistical procedure is kriging, which was developed by Matheron in 1963. Kriging is a family of generalized least-squares regression algorithms. Ordinary kriging is a well-known member of the kriging family that uses only the sampled primary variable to make estimates at unsampled locations. Cokriging allows one or more secondary or ancillary variables to be included in the model and assuming that the primary and ancillary variables are moderately correlated, the estimation accuracy of the primary variable should increase. In this paper, we compare two different types of geostatistical procedures, ordinary kriging and three cokriging procedures, for making a continuous map. In a subsequent study, we plan to apply our stratification equations to these results. The primary variable for both ordinary kriging and cokriging is cubic foot volume per acre. The secondary variable is calculated from Landsat Thematic Mapper (TM) satellite imagery. This is an exhaustive data set and allows for a thorough investigation of the spatial autocorrelation between the primary and secondary variables.

## DATA

The cubic foot volume data came from the 1998 inventory for Connecticut conducted by the Northeastern Forest Inventory and Analysis unit (NEFIA) of the USDA Forest Service. Forest inventories are designed to estimate the amount of forest area and total volume to within a specified statistical error. The sampling design is double sampling for stratification (Cochran 1977). For the first phase sample of Connecticut, 12,132 systematically located points were photo interpreted for land cover. The forested plots were further photo interpreted for volume class estimates, which were used for stratification. Sample forested ground plots are selected proportional to the photo interpreted volume class. Both forest and nonforest plots are included in the on-the-ground or second phase sample. The NEFIA plot design is a cluster of four circular plots each with a 24 ft radius. The center of one circular plot is co-located with the cluster center and the remaining three plots are located 120 feet from the plot center and 120° apart. This study used 452 clusters with an average distance between the clusters of approximately 3 km. NEFIA refers to the cluster as a plot. All of the trees within the boundaries of the plots were measured. Only live trees larger than 5 inches in diameter at breast height (dbh) were included in this study. The cubic foot volume of all of these trees was summed for a cluster total and put on a per acre

basis. Figure 1 shows the distributions of the forested clusters by five volume classes across the state of Connecticut. NEFIA has fewer clusters or plots in the area surrounding New York City than in any other part of the state. Low volume clusters are found surrounding the I-91 corridor, which runs through the middle of the state from New Haven through Hartford into Massachusetts. There is a concentration of high volume clusters in the northwestern part of the state which is mountainous and the least developed region of the state. The remaining parts of the state have a mixture of volume classes.

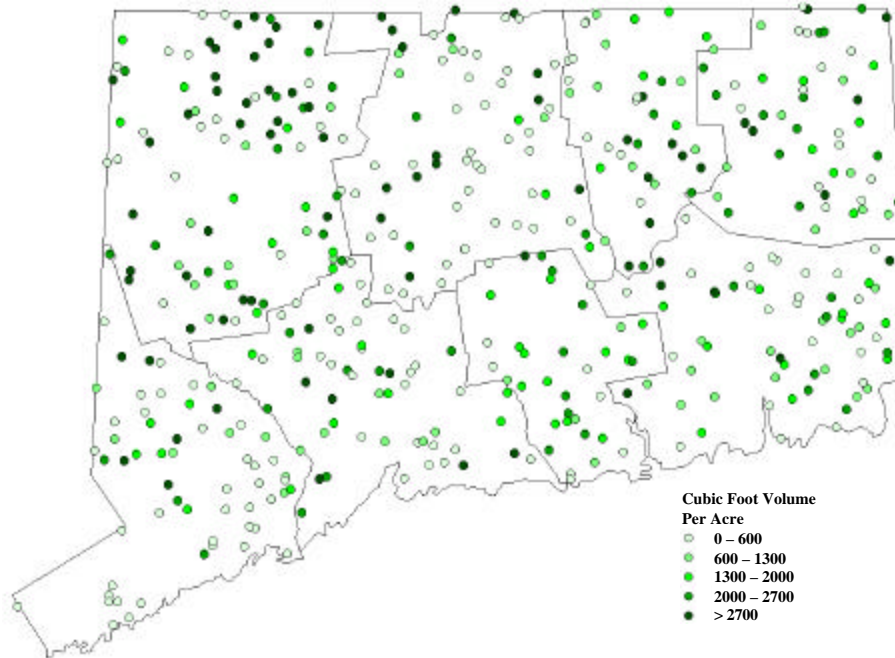


Figure 1. Map of the distribution of volume classes across Connecticut. The lower volume classes are around New York City and the I-91 corridor, which runs through the middle of the state. There is a concentration of higher volume classes in the northwestern part of the state.

The secondary variable is the normalized difference vegetation index (NDVI), which was calculated from an August 1996 TM satellite imagery scene. TM sensors measure the energy reflected off 30 m square blocks of area (pixels) over the landscape in seven spectral bands. Three bands are in the visible, one in the infrared, two in the middle infrared, and one in the thermal portion of the spectrum. The reflectance of each 30 x 30 m pixel is recorded as a digital number (DN) between 0 and 256. Each pixel has seven DN's, one for each band. NDVI is a commonly used vegetation index that is highly correlated with green biomass. It is based on the green plant cell high reflectance of the near infrared wavelength and low reflectance of the red wavelength Metzger 1997, Jensen 1996). NDVI is computed as follows:

$$NDVI = \frac{NIR - Red}{NIR + Red} \quad (1)$$

where NIR is the radiance in the near-infrared (0.76 – 0.90  $\mu\text{m}$ ) and Red is the radiance in the red (0.63 – 0.69  $\mu\text{m}$ ) part of the spectrum. NDVI ranges from –1 to 1 and can be rescaled to be between 0 and 255.

There are more than 25 million 30 x 30 m pixels in the state of Connecticut. Figure 2 shows the spatial arrangement of our ground plots vs. 30 m TM pixels. One of the four circular plots may be located on more than one pixel. Due to the resolution mismatch of the plots vs. the pixels, locational uncertainties due to the Geographic Positioning System (used to locate the plots), and to image registration errors, we averaged the nine NDVI values within a 90 x 90 m pixel and reported the average back to the center of the pixel. This procedure is applied to all of the pixels in the state.

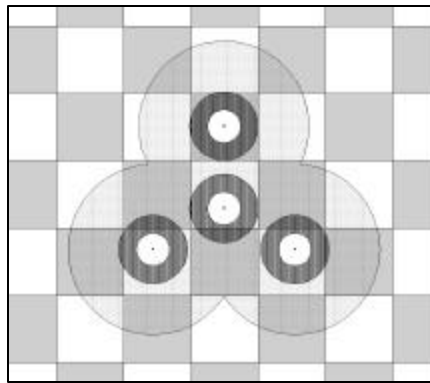


Figure 2. Map of the FIA ground plots superimposed on 30 m pixels. The FIA plot design is a cluster of four 24-foot radius plots. The dark gray circles correspond to areas of locational uncertainty due to GPS errors. The cloverleaf area corresponds to an area of locational uncertainty due to image restoration errors.

## MODELS OF SPATIAL CONTINUITY

Kriging and cokriging require a model of spatial continuity. The three most common models of spatial continuity are the variogram or semivariogram, covariance, and correlogram, which are used to model the average degree of similarity or dissimilarity as a function of both distance and direction. All three models of spatial continuity should be investigated because they may produce different results depending on the data. The skewness, the spatial arrangement of the samples, the change of local variability of the data across the study area or

heteroscedasticity, and preferential clustering of samples all impact the model of spatial continuity. It is difficult to discern *a priori* the impact of the data on the model. Rossi *et al.* (1992, 1994), Liebhold *et al.* (1993), Goovaerts (1997), Isaaks and Srivastava (1989), and others discuss these models of spatial continuity. The term variogram and semivariogram are often interchanged. A semivariogram is one-half of the lag variance that is reported in the variogram. Furthermore, variogram or semivariogram are often used as generic terms for the model of spatial continuity.

Let  $z(\mathbf{u}_i)$  represent the value of the attribute  $z$  at location  $\mathbf{u}_i$ . Let  $z(\mathbf{u}_i + \mathbf{h})$  represent the value of the same attribute  $\mathbf{h}$  distance (lag units) apart and in a particular direction. Unless the observations are on a grid, there are very few observations exactly  $\mathbf{h}$  lags apart from  $z(\mathbf{u}_i)$ . Therefore, all observations within a specified lag and angle tolerance are included in the number of pairs,  $N(\mathbf{h})$ . Datum  $z(\mathbf{u}_i)$  is the tail and  $z(\mathbf{u}_i + \mathbf{h})$  is the head of the vector. Means and standard deviations of the tail and head are:  $m_{z(\mathbf{u}_i)}$ ,  $\sigma_{z(\mathbf{u}_i)}^2$ ,  $m_{z(\mathbf{u}_i + \mathbf{h})}$ , and  $\sigma_{z(\mathbf{u}_i + \mathbf{h})}^2$ . The semivariogram  $\gamma(\mathbf{h})$ , covariance  $C(\mathbf{h})$ , and correlogram function  $\rho(\mathbf{h})$  are given below in equations 2-4.

$$\gamma(\mathbf{h}) = \frac{1}{2N(\mathbf{h})} \sum_{i=1}^{N(\mathbf{h})} [z(\mathbf{u}_i) - z(\mathbf{u}_i + \mathbf{h})]^2 \quad (2)$$

$$C(\mathbf{h}) = \frac{1}{N(\mathbf{h})} \sum_{i=1}^{N(\mathbf{h})} [z(\mathbf{u}_i) - m_{z(\mathbf{u}_i)}] [z(\mathbf{u}_i + \mathbf{h}) - m_{z(\mathbf{u}_i + \mathbf{h})}]$$

where

$$m_{z(\mathbf{u}_i)} = \frac{1}{N(\mathbf{h})} \sum_{i=1}^{N(\mathbf{h})} z(\mathbf{u}_i) \quad \text{and} \quad m_{z(\mathbf{u}_i + \mathbf{h})} = \frac{1}{N(\mathbf{h})} \sum_{i=1}^{N(\mathbf{h})} z(\mathbf{u}_i + \mathbf{h})$$

$$\rho(\mathbf{h}) = \frac{C(\mathbf{h})}{\sqrt{\sigma_{z(\mathbf{u}_i)}^2 \sigma_{z(\mathbf{u}_i + \mathbf{h})}^2}}$$

where

$$\sigma_{z(\mathbf{u}_i)}^2 = \frac{1}{N(\mathbf{h})} \sum_{i=1}^{N(\mathbf{h})} [z(\mathbf{u}_i) - m_{z(\mathbf{u}_i)}]^2 \quad \text{and} \quad \sigma_{z(\mathbf{u}_i + \mathbf{h})}^2 = \frac{1}{N(\mathbf{h})} \sum_{i=1}^{N(\mathbf{h})} [z(\mathbf{u}_i + \mathbf{h}) - m_{z(\mathbf{u}_i + \mathbf{h})}]^2 \quad (4)$$

Both the covariance and correlogram are measures of similarity, whereas the semivariogram is a measure of dissimilarity. As the lag or distance increases, the covariance and the correlogram decrease, whereas the variogram increases. Under mathematical conditions of second-order stationarity, the semivariogram, correlogram, and covariance may be expressed in terms of each other. Since cokriging uses ancillary data, a variogram is required for the secondary variable as well as the primary variable. In addition, cross variograms are required between the primary and all secondary variables.

The cross model of spatial continuity measures the cross dependence between two different attributes  $z_i$  and  $z_j$ . (Goovaerts 1997, Isaaks and Srivastava 1989, and Pannatier 1996). The cross semivariogram  $\gamma_{ij}(\mathbf{h})$ , cross-covariance  $C_{ij}(\mathbf{h})$ , and cross-correlogram  $\rho_{ij}(\mathbf{h})$  are given in equations 5-7.

$$\gamma_{ij}(\mathbf{h}) = \frac{1}{2N(\mathbf{h})} \sum_{\mathbf{z}_i, \mathbf{z}_j} (z_i(\mathbf{u}) - \mu_i)(z_j(\mathbf{u} + \mathbf{h}) - \mu_j) \quad (5)$$

$$C_{ij}(\mathbf{h}) = \frac{1}{N(\mathbf{h})} \sum_{\mathbf{z}_i, \mathbf{z}_j} (z_i(\mathbf{u}) - \mu_i)(z_j(\mathbf{u} + \mathbf{h}) - \mu_j) \quad (6)$$

where

$$m_{i+\mathbf{h}} = \frac{1}{N(\mathbf{h})} \sum_{\mathbf{z}_i} z_i(\mathbf{u}) \quad \text{and} \quad m_{j+\mathbf{h}} = \frac{1}{N(\mathbf{h})} \sum_{\mathbf{z}_j} z_j(\mathbf{u} + \mathbf{h})$$

$$\rho_{ij}(\mathbf{h}) = \frac{C_{ij}(\mathbf{h})}{\sqrt{\sigma_{i-\mathbf{h}}^2 \sigma_{j+\mathbf{h}}^2}}$$

where

$$\sigma_{i-\mathbf{h}}^2 = \frac{1}{N(\mathbf{h})} \sum_{\mathbf{z}_i} (z_i(\mathbf{u}) - \mu_i)^2 \quad \text{and} \quad \sigma_{j+\mathbf{h}}^2 = \frac{1}{N(\mathbf{h})} \sum_{\mathbf{z}_j} (z_j(\mathbf{u} + \mathbf{h}) - \mu_j)^2 \quad (7)$$

The mean and variance of tail,  $z_i(\mathbf{u})$ , and head,  $z_j(\mathbf{u} + \mathbf{h})$ , of the vector are:  $m_{i-\mathbf{h}}$ ,  $\sigma_{i-\mathbf{h}}^2$ ,  $m_{j+\mathbf{h}}$ , and  $\sigma_{j+\mathbf{h}}^2$ .

The models of spatial continuity developed from the sample data are experimental models. The experimental models are fitted with a theoretical model and it is the theoretical model that is inserted into the kriging, cokriging, and other geostatistical models. Exponential, Gaussian, spherical, and their linear combinations are routinely used as theoretical models because they satisfy a positive definiteness requirement in the kriging and cokriging equations.

All experimental and theoretical variograms have a range and a nugget and many rise and then level off at the sill. The sill is the population variance or the correlation coefficient in the case of the cross-semivariogram. Often the semivariogram is standardized by dividing each semivariogram value by the product of the head and tail standard deviations. The product of the head and tail standard deviations should be close to the population variance. For a standardized semivariogram, the sill should be approximately 1. The distance at which the semivariogram reaches its sill is called the range. Since the exponential and Gaussian models reach their sill asymptotically, the distance at which 95% of the sill is reached is referred to as the practical

range. Beyond the range, the samples are no longer correlated and are thus independent. The intercept of the semivariogram on the vertical axis is called the nugget. Ideally, the nugget should be zero. A nonzero nugget indicates spatial variability below the minimum lag, which cannot be measured with the current sampling scheme, sampling error, or both. Correlograms and covariance functions which are not expressed in variogram form have a nugget equal to population variance and a sill of zero.

## COKRIGING MODELS

Both kriging and cokriging minimize the prediction variance subject to unbiasedness constraints. This nonlinear system is solved using Lagrange multipliers. Atkinson *et al.* (1992, 1994), Bourgault and Marcotte (1991), Dungan (1998), Goovaerts (1994a, 1997, 1998, 1999), Meyers (1991), and Wackernagel (1995) are excellent references on cokriging. In cokriging, the solution is based on the joint distribution of the primary and secondary variables. For a single primary variable P and a single secondary variable S, the following covariance matrix must be positive definite. The theory for solving kriging and cokriging systems was originally developed for the covariance function but has been extended to the semivariogram and correlogram.

$$\begin{bmatrix} C_{PP} & C_{PS} \\ C_{SP} & C_{SS} \end{bmatrix} \quad (8)$$

Finding valid cross covariance matrices is an active area of research (Goovaerts 1994 b and c, Goulard and Voltz 1992, Yao 1999, and Yao and Journel 1998). The linear model of coregionalization (LMC) is one valid covariance matrix. An LMC requires that every structure in the cross variogram or other model of spatial continuity be included in the model of spatial continuity model for primary and secondary variables. However, the primary and secondary variables may have structures not found in the model of spatial continuity for the cross variogram models. In terms of a semivariogram model, consider the following LMC.

$$\begin{bmatrix} \gamma_{PP} & \gamma_{PS} \\ \gamma_{SP} & \gamma_{SS} \end{bmatrix} = \begin{bmatrix} b_{PP}^0 & b_{PS}^0 \\ b_{PP}^1 & b_{PS}^1 \\ b_{PP}^2 & b_{PS}^2 \end{bmatrix} \begin{bmatrix} \gamma_{h_1} \\ \gamma_{h_2} \\ \gamma_{h_3} \end{bmatrix} \quad (9)$$

The two direct semivariograms,  $\gamma_{PP}$  and  $\gamma_{SS}$ , and the cross semivariogram,  $\gamma_{PS}$ , are defined in terms of the structure,  $\gamma_{h_1}$ . The semivariogram of the primary variables has an additional structure,  $\gamma_{h_2}$ . The nuggets for the primary variogram, cross variogram, and secondary variogram are respectively,  $b_{PP}^0$ ,  $b_{PS}^0$ , and  $b_{SS}^0$ . The weights for the other structures are:  $b_{PP}^1$ ,  $b_{PS}^1$ ,  $b_{SS}^1$ , and  $b_{PP}^2$ . The three structure LMC model is.

$$\begin{bmatrix}
 b_{PP}^0 & b_{PS}^0 & 0 \\
 b_{PS}^0 & b_{SS}^0 & 0 \\
 0 & 0 & 0
 \end{bmatrix}
 \begin{bmatrix}
 \mathbf{h}_1 \\
 \mathbf{h}_2 \\
 \mathbf{h}_3
 \end{bmatrix}
 +
 \begin{bmatrix}
 b_{PP}^1 & b_{PS}^1 & 0 \\
 b_{PS}^1 & b_{SS}^1 & 0 \\
 0 & 0 & 0
 \end{bmatrix}
 \begin{bmatrix}
 \mathbf{h}_1 \\
 \mathbf{h}_2 \\
 \mathbf{h}_3
 \end{bmatrix}
 +
 \begin{bmatrix}
 b_{PP}^2 & b_{PS}^2 & 0 \\
 b_{PS}^2 & b_{SS}^2 & 0 \\
 0 & 0 & 0
 \end{bmatrix}
 \begin{bmatrix}
 \mathbf{h}_1 \\
 \mathbf{h}_2 \\
 \mathbf{h}_3
 \end{bmatrix}
 \quad (10)$$

Since each of the above matrices is symmetric,  $b_{SP}^\square = b_{PS}^\square$ , for all  $\square$  structures and

$b_{PP}^\square = b_{SS}^\square$  (Goovaerts 1997). Each matrix must be positive definite, i.e.,  $b_{PP}^\square, b_{SS}^\square, b_{PS}^\square$  and have nonnegative diagonal elements.

For a primary and a single secondary variable, there are two variograms and one cross variogram to model. If there is a primary variable and two secondary variables, then there are six models of spatial continuity to construct. Generally, the primary and secondary variables do not have the same range and finding coefficients that meet the positive definite requirements is difficult. Computer algorithms for solving the LMC are given in Morissette (1997), Goulard (1989), and Goovaerts (1997).

Markov Model 1 (MM1) and Markov Model 2 (MM2) (Almeida and Journel 1994, Journel 1999, Ma and Journel 1999, and Shmaryan and Journel 1999) are two Markov models which screen the data, eliminating the building of a full linear model of coregionalization as described above. These models are applicable in the case of dense secondary data, which is often found in practice, and is certainly the case with satellite data. The secondary datum closest to the primary variable is relocated to coincide with the primary variable. Hence the name collocated cokriging. Collocated cokriging results in a smaller and faster model. In the Markov model proposed by Almeida and Journel (1994), MM1, only a model of spatial continuity is required for the primary variable. The secondary covariate function is not required in the cokriging system. Only the stationary secondary variance is required. The model of spatial continuity for the cross semivariogram is inferred as follows.

$$\gamma_{PS}(h) = \sqrt{\frac{C_{SS}(0)}{C_{PP}(0)}} \gamma_{PS}(0) + \gamma_{PP}(h) \quad (11)$$

$C_{PP}(0)$  is the sill of the  $\gamma_{PP}(h)$  model and since the secondary semivariogram is not modeled  $C_{SS}(0)$  is the population variance of the secondary variable. The correlation coefficient of the collocated variables is  $\gamma_{PS}(0)$ . The semivariogram of the primary variable is assumed to be proportional to the cross semivariogram and this assumption should be verified (Goovaerts 1997). Ma and Journel (1999) state that the collocated primary datum screens the influence of any primary data located further away on the secondary variable. This screening hypothesis makes sense if the volume support of the primary variable is larger and includes that of the secondary variable.

According to Ma and Journel (1999), in applications involving remote sensing secondary data, the volume support of the secondary data is typically larger than the primary variable. The

screening effect would be opposite that of the MM1 model. Beginning with a model of spatial continuity for the secondary variable, the cross semivariogram is modeled as follows.

$$\gamma_{PS}(h) = \sqrt{\frac{C_{PP}(0) - \gamma_{SS}(h)}{C_{SS}(0)}} \gamma_{PS}(0) + \gamma_{SS}(h) \quad (12)$$

Here  $C_{PP}(0)$  is the primary sample variance and  $C_{SS}(0)$  is the sill of  $\gamma_{SS}(h)$  model. The MM2 cross semivariogram has a lower nugget than the model provided by either LMC or MM1 because it is modeled from  $\gamma_{SS}(h)$  which is based on an exhaustive sample and hence has a low nugget. This new model introduced by Journel (1999) is called MM2. This time, the collocated secondary datum screens the influence of other secondary data located further away on the primary variable. In addition to estimating a cross model of spatial continuity, the primary model of spatial continuity is also estimated as a linear combination of the secondary variance model and a reference variogram  $\gamma_R(h)$  with unit sill.

$$\gamma_{PP}(h) = C_{PP}(0) \gamma_{PS}(0) + \frac{\gamma_{SS}(h)}{C_{SS}(0)} \gamma_{PS}(0) + \gamma_{PS}(0) \gamma_R(h) \quad (13)$$

$C_{PP}(0)$  and  $C_{SS}(0)$  are the primary and secondary variances. In practice,  $\gamma_R(h)$  is modeled from the experimental difference values (Ma and Journel 1999). Equations 12 and 13 plus the variogram for the secondary variable provide the models for an LMC (Journel 1999).

GSLIB (Deutsch and Journel 1998) is public domain software for geostatistics. The program kt3d from this package is used for ordinary kriging. The GSLIB software package has a program for cokriging, but it does not have either the MM1 or MM2 options. Ma and Journel (1999) wrote an extension of the GSLIB subroutine to include MM1 and MM2 and the software is available at <http://www.iamg.org>.

## ERROR ASSESSEMENT

Root mean square error, overall accuracy in a confusion matrix, and the kappa statistic were selected to compare kriging with the three cokriging procedures. The original data as well as the two estimated data sets were assigned to one of the five volume classes. A confusion or error matrix was constructed comparing kriging estimates with the ground truth and another compared cokriging estimates with ground truth. The sum of the diagonal matrix elements divided by the total number of observations multiplied by 100% equals the overall accuracy. This statistic does not capture the closeness of the misclassifications to the correct classification class. The kappa statistic is a measure of the agreement beyond that expected by chance alone between two or more raters. Here one rater is the observed cubic foot volume, or ground truth, and the other rater is the classification model. Kappa ranges usually from 0 to 1, although

negative values are possible. A value of 1 indicates perfect agreement while a value of 0 indicates no additional agreement than that expected by chance. A negative value for kappa indicates agreement which is less than that expected by chance. Landis and Koch (1977) classified different ranges of kappa. These classifications are poor ( $\kappa < 0.4$ ), good ( $0.4 < \kappa < 0.75$ ) and excellent ( $\kappa > 0.75$ ).

To validate the results, the original data set is split into a model and a validation data set by selecting with a random number generator 80% of the sample data for the model data set and the remaining 20% of the data for the validation data set. This was repeated 25 times, generating a different model and validation data set for each trial.

## RESULTS AND DISCUSSION

Figure 3 is a histogram of the distribution of the clusters by five volume classes. These volume classes are used to classify the estimated values from kriging and cokriging. Approximately 40% of the clusters are in the 0-600 cubic foot volume class. This includes nonforested clusters. The remaining four classes are evenly distributed each containing approximately 15% of the clusters. The average cubic foot volume was 1353 cubic feet per acre.

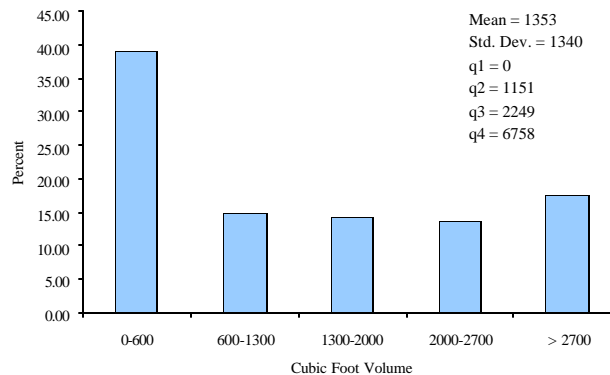


Figure 3. Histogram and univariate statistics for the primary variable, cubic foot volume. Approximately 40% of the clusters are in the lowest volume class, which includes nonforested plots.

Figure 4 shows the histogram of NDVI for the 2,351,104 pixels in Connecticut. All of the 51 classes have members. However, many class sizes are too small to be graphed. For example, the 250-255 class has 850 members, which is approximately 0.04% of the total pixels. Hoppus *et al.* (in press) found that the NDVI value which best discriminates forest from nonforest land was around 235. Approximately 41.8% of the pixels have an NDVI of 230 or larger. The large number of pixels with a NDVI of 0 is due to bodies of water and the large number of pixels with a NDVI between 105 and 130 correspond to ploughed fields.

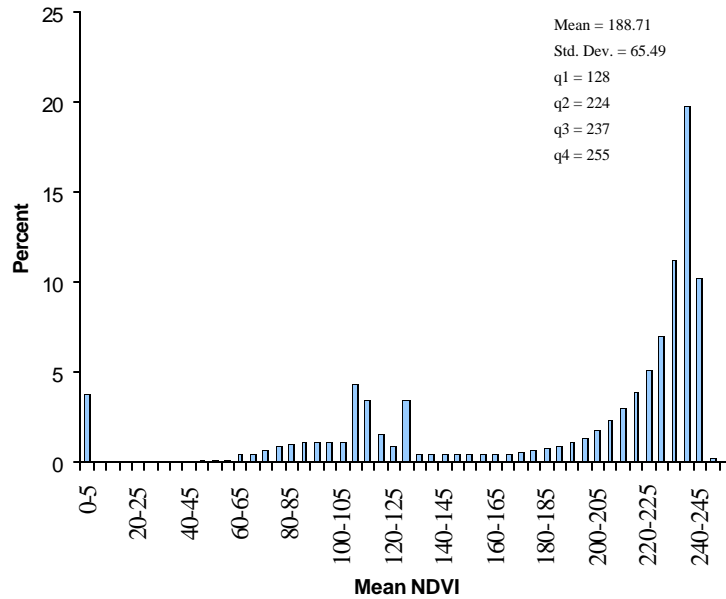


Figure 4. Histogram and univariate statistics for the secondary variable, mean NDVI, for 2,351,104 pixels. Approximately 25% of the pixels are above the forest/nonforest NDVI threshold of 235.

The relationship between the primary variable, cubic foot volume, and the secondary variable, NDVI, is important in cokriging. Figure 5 shows the scattergram of the collocated primary and secondary variables. The Pearson correlation coefficient is 0.416 with a  $p = 0.0001$  and the Spearman rank correlation is 0.579 with a  $p = 0.0001$ . The linear relationship between cubic foot volume and NDVI is moderately strong. As expected, observations with lower NDVI have lower volume values. There is a spike of high volume for NDVI values between 230 and 240.

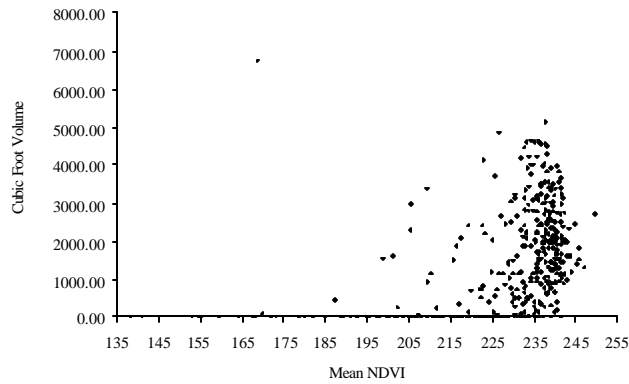


Figure 5. Scattergram of collocated primary and secondary variables. The correlation coefficient is 0.416 and there is a spike of high volume clusters around the forest/nonforest NDVI threshold of 235.

Figure 6(a) shows the experimental and theoretical standardized semivariogram for cubic foot volume used in kriging. The estimated experimental semivariogram,  $\hat{\gamma}(\mathbf{h})$ , is fitted using an exponential function given in equation 14.

$$\hat{\gamma}_{\text{volume}}(\mathbf{h}) = 0.758 + 0.254 \left( 1 - \exp\left(-\frac{3 \|\mathbf{h}\|}{31,176}\right) \right) \quad (14)$$

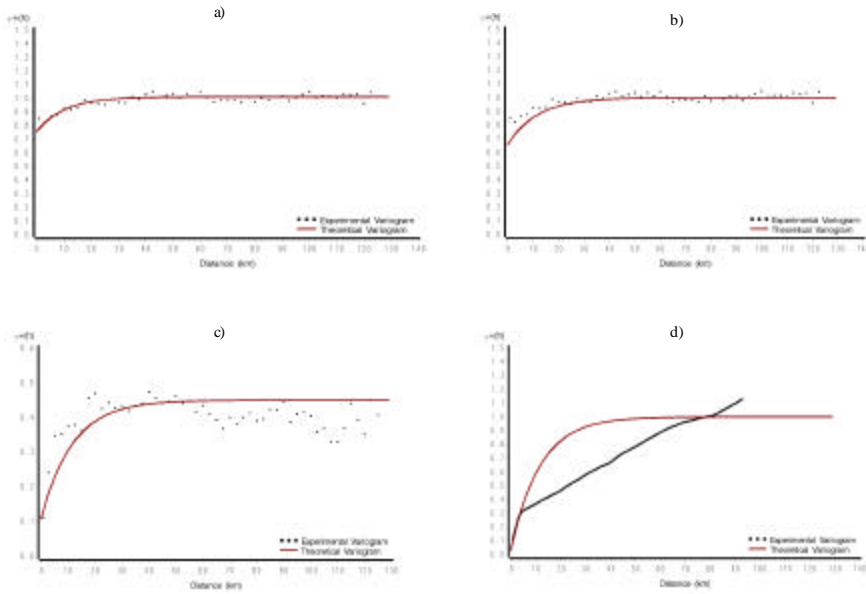


Figure 6. Experimental and theoretical semivariograms for: (a) the primary variable, cubic foot volume, used in kriging; (b) the primary variable, cubic foot volume, used in cokriging; (c) the cross-variogram between the primary and secondary variable used in cokriging; and (d) the secondary variable, mean NDVI, used in cokriging. The experimental variogram appears as a solid line for NDVI due to the exhaustive secondary data set. The lag distance is shorter and there are more observations. All of the semivariograms are omnidirectional.

The semivariogram has a nugget of 0.758 and a practical range of 31,176 m and the sill is one since the semivariogram was normalized. The semivariogram for cubic foot volume, the cross semivariogram between cubic foot volume and mean NDVI for the 452 collocated observations, and the semivariogram for NDVI mean are shown in Figures 6(b), (c), (d). The fitted theoretical variograms given in equations 15-17, respectively.

$$\gamma_{volume}^*(h) = 0.657 + 0.343 \left( 1 - \exp\left(-\sqrt{3} \frac{h}{34,987}\right) \right) \quad (15)$$

$$\gamma_{NDVI}^*(h) = 0.108 + 0.342 \left( 1 - \exp\left(-\sqrt{3} \frac{h}{34,987}\right) \right) \quad (16)$$

$$\gamma_{volume \& NDVI}^*(h) = 0.039 + 0.960 \left( 1 - \exp\left(-\sqrt{3} \frac{h}{34,987}\right) \right) \quad (17)$$

All three theoretical semivariograms have the same range, 34,987 m, and are fitted using exponential functions. The LMC model was fitted using nonlinear regression, nonlinear programming, and user judgment. None of the three semivariograms is an individual optimal fit

as seen by comparing the semivariograms in Figures 6(a) and 6(b). The optimal fitting cross semivariogram has a range of 13,962 m, a nugget of 0.110, and a sill of 0.427. The sill is close to the correlation coefficient of 0.416. The variogram for NDVI was computed using gam, a regularly spaced variogram procedure from GSLIB, and fitted using nonlinear programming. The theoretical and experimental variogram in Figure 6(d) closely match each other for short lag distances, which is more important because observations closer together should be more similar than those farther apart. The experimental variogram is optimally fitted using a power model, which is not allowed in cokriging because it does not have a sill. Similarly, using the acceptable combination of structures, the variogram for NDVI could be better fitted using two exponential structures with ranges of 2,945 m and 119,294 m. All of the variograms in Figure 6 are omnidirectional. That is, they have an angle tolerance of 90°. We checked for anisotropy, but found it to be insignificant. In the LMC, the common structures would be required to have the same anisotropy.

Table 1 shows the results for ordinary kriging and the three cokriging models. MM2 has the lowest mean square error, the highest number of correct matches, and the highest kappa statistic. This agrees with the results from the literature. Although poor, the kappa statistic is twice as high for MM2 as for the other procedures. LMC was inferior to ordinary kriging. The mean, standard deviation, and quartile breaks are lower for all of the procedures than for the sample population.

Table 1. The comparison statistics for kriging and three cokriging procedures using all 452 clusters.

Procedure	RMSE	Overall		Mean	Standard					
		Accuracy	Kappa		Deviation	Minimum	Q1	Q2	Q3	Q4
Kriging	1069.94	28.76	0.14	1273.91	565.05	0.00	930.09	1277.02	1595.62	3450.54
LMC	1093.45	19.25	0.05	1303.84	346.83	498.32	1062.61	1289.18	1503.56	2829.53
MM1	1047.09	28.98	0.14	1257.59	538.58	7.59	902.39	1241.47	1573.20	3452.49
MM2	752.12	45.80	0.33	1289.87	578.30	24.59	924.89	1212.92	1603.02	4065.50

Figures 7(a) and (b) show that MM2, the superior procedure, is tighter around the 45° line. Both procedures overestimate low cubic foot volume clusters and underestimate high cubic foot volume clusters. The break point is approximately the sample mean, indicating that both procedures perform better near the sample mean and worse towards the tails of the distribution. Figures 8(a) and (b) map the estimated values for kriging and MM2. Both maps show high cubic foot volume in the mountainous northwestern portion of the state and low cubic foot volume in the New York City area and along the I-91 corridor. The map for MM2 reveals fine scale heterogeneity, which is characteristic of the satellite data. Figure 8c is a map of the difference (cokriging – kriging) between the two procedures. The map does not reveal any spatial patterns indicating regions in which one procedure is superior to the other.

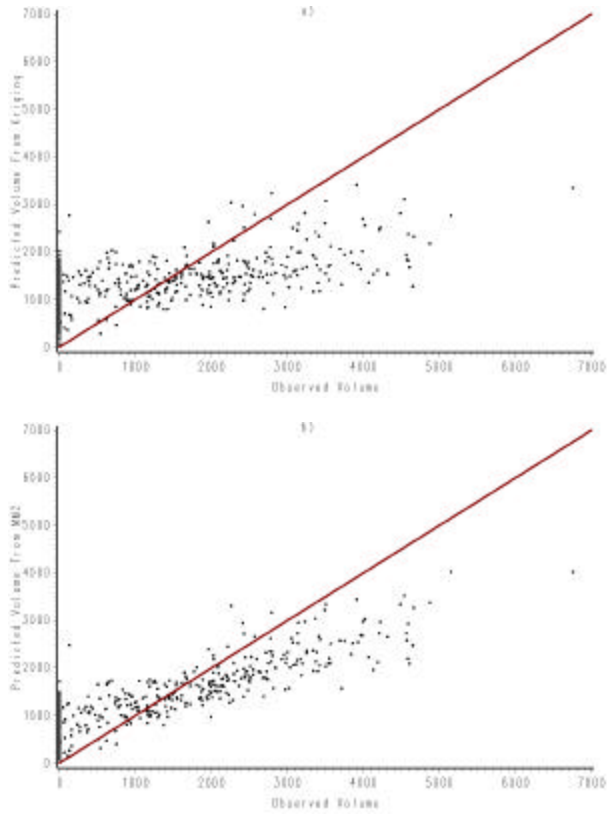


Figure 7. Estimated values vs. the sample observations for: (a) kriging and (b) cokriging. The 45° line is in red. MM2 is clearly superior to kriging since it has a tighter fit around the 45° line. The tightest fit is near the sample mean for cubic foot volume. Below the sample mean both procedures overestimate cubic foot volume and above the sample mean, the two procedures underestimate cubic foot volume.

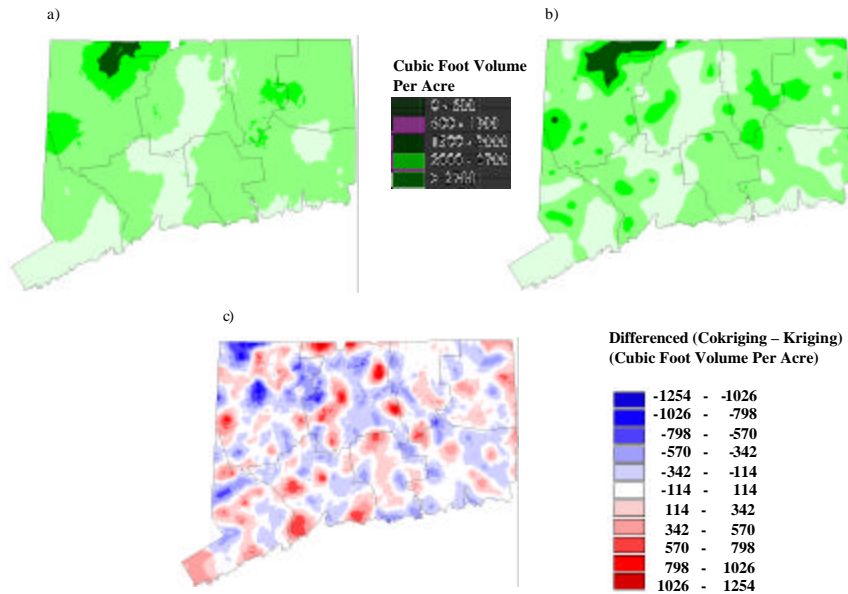


Figure 8. Maps of the estimated values from: (a) kriging; (b) MM2 cokriging procedure; and (c) the difference of the two estimates (cokriging-kriging). Both maps reveal the same large-scale features: low volume around New York City and the I-91 corridor and high volume in the mountainous, undeveloped northwestern region of the state. However, the MM2 cokriging map reveals fine scale heterogeneity, whereas the cokriging map is smooth. The difference map does not indicate any geographic regions in which one procedure is superior to the other.

The above procedure was repeated 25 times, generating a different model and validation data set for each trial. Both kriging and MM2 were applied to each model data set. Using the validation dataset, the predicted values were compared with the observed values. The RMSE, overall accuracy, and the kappa statistic are found in Table 2. In 19 of the validation data sets, MM2 is clearly superior and the two procedures tie in two cases. As expected, the same trend occurred for the kappa statistic. In 17 of the validation data sets, MM2 is superior and the two procedures tied in 4 data sets. For the mean of the 25 cross-validations, the same pattern occurs, *e.g.*, the RMSE, overall accuracy, and kappa are higher for MM2. Unlike the model with all 452 sample points, the 25 cross-validation models show that kriging has a lower RMSE than cokriging. An analysis of the residuals did not reveal any patterns that would explain this discrepancy. We mapped the volume class differences between the estimated and predicted values for several validation data sets and found no spatial trend. The zero, one, two, three, or four differences were not clustered in a particular geographic area. With regard to class differences, an examination of the confusion matrices reveals that MM2 more accurately classifies low cubic foot volume, 0 - 600, and high cubic foot volume classes,  $> 2700$ . Kriging may fail to correctly classify any estimated values in the latter class.

Table 2. The cross-validation comparison statistics for kriging and the MM2 cokriging procedure.

Validation number	Number of observations in validation data	-----Kriging-----			-----MM2-----		
		RMSE	Overall Accuracy	Kappa	RMSE	Overall Accuracy	Kappa
1	108	1231.16	21.30	0.048	1254.80	23.15	0.068
2	87	1287.39	24.14	0.106	1310.56	25.29	0.114
3	94	1312.89	18.09	0.040	1396.06	23.40	0.093
4	85	1273.77	23.53	0.071	1296.49	23.53	0.067
5	87	1326.00	22.99	0.064	1336.54	20.69	0.035
6	93	1237.32	20.43	0.040	1290.24	26.88	0.113
7	93	1240.42	20.43	0.050	1320.64	29.03	0.139
8	95	1363.06	25.26	0.124	1355.44	27.37	0.129
9	104	1331.53	24.04	0.068	1387.13	24.04	0.066
10	97	1274.65	23.71	0.071	1306.53	29.90	0.137
11	83	1269.53	16.87	-0.001	1360.22	21.69	0.045
12	95	1257.85	20.00	0.071	1350.85	23.16	0.077
13	86	1234.89	22.09	0.062	1241.09	20.93	0.031
14	89	1222.73	23.60	0.048	1278.70	23.60	0.047
15	108	1302.40	28.70	0.135	1336.31	23.15	0.062
16	90	1317.19	18.89	0.034	1355.37	21.11	0.051
17	93	1223.60	19.36	0.014	1266.56	33.33	0.164
18	98	1360.51	20.41	0.058	1381.94	26.53	0.116
19	95	1401.07	13.68	0.020	1469.81	21.05	0.059
20	88	1358.08	17.05	0.017	1448.66	20.46	0.047
21	86	1251.49	17.44	0.004	1278.88	22.09	0.050
22	81	1431.29	14.82	0.022	1432.04	20.99	0.078
23	80	1215.92	22.50	0.066	1274.56	23.75	0.062
24	81	1243.49	24.69	0.096	1296.24	23.46	0.073
25	87	1108.23	20.69	0.072	1381.30	24.14	0.095
mean	91.32	1283.06	20.99	0.056	1336.28	24.11	0.081

In conclusion, the overall accuracy and the kappa statistic indicate that the MM2 cokriging procedure is a superior classifier for the five volume classes than ordinary kriging. It would be interesting to determine the impact of both more sampling data and the systematic hexagonal grid structure that will be used in the new nationwide annualized inventory. In this study, the spatial arrangement of the data did not appear to play a crucial role. Otherwise, there would be greater swings in the validation data set results.

In the future, we plan to look at other vegetation indices including tasseled cap and Landsat TM band 4 and several surrogate variables for volume. The impact of sapling stands should also be considered. Our results will be compared with k-Nearest Neighbors; another technique for producing wall-to-wall maps. We plan to investigate other geostatistical techniques including kriging with a trend model.

The final kriging or cokriging map has over 2.3 million grid cell estimates. Even though sample data has been used to create these maps and the final grid cell estimates corresponding to the 452 clusters are correlated, the grid cell estimates could possibly be used in post

stratification. This is an important issue as all of the FIA units across the country are moving to an annual inventory and will be investigated. The ground sampled plots will be on a systematic hexagonal grid in the annual inventory and the phase one sample will be conducted using satellite imagery and not aerial photography. The volume class estimates will be from either satellite imagery or the output from cokriging or another continuous mapping procedure. This information will be used in post-stratification since the plots will be either current plots or new plots located at the hexagonal center.

### LITERATURE CITED

- Almeida, A.S. and A.G. Journel. 1994. Joint simulation of multiple variables with a Markov-type coregionalization model. Mathematical Geology 26(5):565-588.
- Atkinson, P.M., R. Webster, and P. J. Curran. 1994. Cokriging with airborne MSS imagery. Remote Sens. Environ. 50:335-345.
- Atkinson, P.M., R. Webster, and P.J. Curran. 1992. Cokriging with ground-based radiometry. Remote Sens. Environ. 41:45-60.
- Bourgault, G. and D. Marcotte. 1991. Multivariable variogram and its application to the linear model of coregionalization. Mathematical Geology 23(7):899-928.
- Cochran, W.G. 1977. *Sampling Techniques*. John Wiley & Sons, Inc., New York. 428p.
- Deutsch, C.V. and A.G. Journel. 1998. *GSLIB Geostatistical Software Library and User's Guide, Second Edition*. Oxford University Press, New York. 369p.
- Dungan, J. 1998. Spatial prediction of vegetation quantities using ground and image data. Int. J. Remote Sensing 19(2):267-285.
- Goovaerts, P. 1999. Performance comparison of geostatistical algorithms for incorporating elevation into the mapping of precipitation. In: Proceedings of the 4<sup>th</sup> International Conference on GeoComputation. Fredericksburg, VA.
- Goovaerts, P. 1998. Ordinary cokriging revisited. Mathematical Geology 30(1):21-42.
- Goovaerts, P. 1997. *Geostatistics For Natural Resources Evaluation*. Oxford University Press, New York.
- Goovaerts, P. 1994a. Study of spatial relationships between two sets of variables using multivariate geostatistics. Geoderma 62:93-107.

- Goovaerts, P. 1994b. On a controversial method of coregionalization. Mathematical Geology 26(2):197-204.
- Goulard, M. 1989. Inference in a coregionalization model. In: *Geostatistics*. M. Armstrong, (ed.). Kluwer, Dordrecht. 397-408.
- Goulard M. and M.Voltz. 1992. Linear coregionalization model: tools for estimation and choice of cross-variogram matrix. Mathematical Geology 24(3):269-286.
- Hoppus, M., R. Riemann, and A. Lister. (In Press). Remote sensing strategies for forest inventory analysis utilizing the FIA plot database. In: Proceedings of RS 2000: Eighth Biennial Remote Sensing Applications Conference. Albuquerque, NM.
- Isaaks, E.H. and R.M. Srivastava. 1989. R.M. *An Introduction to Applied Geostatistics*. Oxford University Press, New York. 561p.
- Jensen, J.R. 1996. *Introductory Digital Image Processing*. Prentice Hall, Upper Saddle River, NJ. 316 p.
- Journel, A.G. 1999. Markov models for cross-covariances. Mathematical Geology 31(8):955-964.
- Landis, J.R. and G.G. Koch. 1977. The measurement of observer agreement for categorical data. Biometrics 33:159-174.
- Liebhold A.M, R.E. Rossi, and W.P. Kemp. 1993. Geostatistics and geographic information systems in applied insect ecology. Annu. Rev. Entomol. 38:303-327.
- Ma, X. and A.G. Journel. 1999. An expanded GSLIB cokriging program allowing for two Markov models. Computers & Geosciences 25:627-639.
- Metzger, K.L. 1997. Modeling forest stand structure to a ten meter resolution using Landsat TM data. M.S. thesis, Department of Forest Sciences, Colorado State University, Fort Collins, CO. 123 p.
- Meyers, D.E. 1991. Pseudo-cross variograms, positive definiteness, and cokriging. Mathematical Geology 23(6):805-817.
- Morisette, J. 1997. Examples using SAS to fit the model of linear model of coregionalization. Computers & Geosciences 23(3):317-323.
- Pannatier, Y. 1996. *Variowin: Software For Spatial Data Analysis in 2D*. Springer-Verlag, New York. 91 p.
- Rossi, R.E., D.J. Mulla, A.G. Journel, and E.H. Franz. 1992. Geostatistical tools for modeling and interpreting ecological spatial dependence. Ecological Monographs 62(2):277-314.

- Rossi, R.E., J.L. Dungan, and L.R. Beck. 1994. Kriging in the shadows: geostatistical interpolation for remote sensing. Remote Sens. Environ. 49:32-40.
- Shmaryan, L.E. and A.G. Journel. 1999. Two Markov models and their application. Mathematical Geology 31(8):965-989.
- Wackernagel, H. 1995. *Multivariate Geostatistics: An Introduction With Applications*. Springer-Verlag, Berlin. 256 p.
- Yao, T. 1999. Nonparametric cross-covariance modeling as exemplified by soil heavy metal concentrations from the Swiss Jura. Geoderma 88:13-38.
- Yao, T. and A.G. Journel. 1998. Automatic modeling of (cross) covariance tables using fast Fourier transform. Mathematical Geology 30(6):589-615.